FROM BASIC RESEARCH TO A PROTOTYPE TOWBODY PLATFORM: PROGRESS ON UNDERWATER UNEXPLODED ORDNANCE REMEDIATION

Kevin L. Williams, Steven G. Kargl, Aubrey L. Espana, Timothy Marston, Daniel S. Plotnick

Applied Physics Laboratory, University of Washington, 1013 NE 40th St., Seattle WA 98105-6698 USA

Steven G. Kargl, Applied Physics Laboratory, University of Washington, 1013 NE 40th St., Seattle WA 98105-6698 USA, FAX: 206-543-1300, kargl@uw.edu

Abstract: *Over the last decade, APL-UW has had an active basic research program to understand the physical mechanisms associated with the scattering of sound from objects near a water-sediment interface. Synthetic aperture sonar (SAS) data were collected during field measurements. A rail was deployed to the bottom, that allowed a mobile sonar tower to traverse an extended cross-range. Inert ordnance, scientific targets, and clutter objects were placed in the field of view. These data were used to validate high-fidelity models, which provided insight into various physical mechanisms observed in the data. Subsequently, the measured data, augmented by numerically simulated data, have been utilized in the development of detection and classification schemes. Our current effort is transitioning the knowledge gained in our basic research to an applied platform. The Multi-Sensor Towbody (MuST) is a prototype platform that integrates commercially available high-frequency side-scan (HF) and downward-looking, low-frequency (LF) sonars with our in-house signal processing package for detection, imaging and classification. The HF sonar provides high-resolution imagery of the water-sediment interface and any proud objects. The LF sonar offers detection depths of 1 to 2 meters (i.e., sand versus mud). This paper discusses the research that has led to design decisions for MuST. [Work supported SERDP, ESTCP, and ONR.]*

Keywords: *Multi-Sensor Towbody, Unexploded ordnance, Synthetic aperture sonar*

1. INTRODUCTION

The Applied Physics Laboratory at the University of Washington (APL-UW) has conducted basic research in the remediation of underwater unexploded ordnance (UXO) for nearly a decade. The primary focus has been the use of low-frequency (LF) synthetic aperture sonar (SAS) in the interrogation of objects near the water-sediment interface. This research included a two pronged approach of field experiments and numerical simulations to gain insight into the physical mechanisms that give rise to unique observable structure in data products derived from sonar data. Examples of data products are the coherent processing of the data to generate SAS images and conversion of data into acoustic colour (AC) templates (i.e., a coloured representation of absolute target strength as a function of frequency and aspect angle).

The transition of our basic research efforts to a prototype sonar platform is described in the remainders of the paper. Section 2 provides brief descriptions of the field experiments that provided data for model validation as well as training and testing data for approaches to the classification problem. Section 3 contains an overview of the numerical models that are used to gain insight into the underlying physical mechanism involved in the acoustic scattering from an object near a water-sediment interface. Signal processing is discussed in Sec. 4, where sonar data are converted to data products suitable for detection and classification schemes. The Multi-Sensor Towbody (MuST) is described in Sec. 5, and its current operational status is provided. Section 6 summarizes.

2. FIELD EXPERIMENTS

Our field experiments can be split into those conducted in a pristine fresh-water pond and those conducted at sea. Pond Experiment 2009 and 2010 (PONDEX09, PONDEX10) are well-controlled experiments where environmental influences (e.g., fish and fouling of objects) were absent. The at-sea field measurements are the Target and Reverberation Experiment 2013 (TREX13), Bay Experiment 2014 (BAYEX14), and the Clutter Experiment 2017 (CLUTTEREX17). These experiments are performed in open waters, and are subject to environmental factors (e.g., fish, shipping noise, weather events, etc.). The significance of each experiment is described below.

PONDEX09 and PONDEX10 were conducted in the test pond facility at the Naval Surface Warfare Center, Panama City Division. The pond is a chlorinated fresh-water pond offering a 17 m depth and medium-fine sand bottom (~1 m thick). A 21-m long rail was deployed, which gave a 19-m SAS aperture. Objects could be placed at 5 to 10 m horizontal ranges from the rail. Sonars were ~4 m above the water-sediment interface on a mobile tower, which moved at 5 cm/s. A sonar transmitted a linear-frequency-modulated (LFM) pulse every 0.5 s. The LFM pulses nominally covered the 1-4, 6-10, 12-28, 30-50, 60-100, and 110-190 kHz bands. PONDEX09 is the initial experiment where data were collected from an isolated UXO (~16-in length, 4-in diameter). Data were also collected from a solid 2:1 aluminum (AL) cylinder (i.e., 2-ft length, 1-ft dia.). The 2:1 AL cylinder has become a canonical reference target as its elastic response to an acoustic field is well understood. PONDEX09 provided proof-of-concept that LF SAS can address the underwater UXO remediation problem [1].

PONDEX10 expanded upon PONDEX09 in three important ways. First, a new sonar spanning the 1-30 kHz band replaced the LF sonars of PONDEX09; thereby increasing the amount of data collected by reducing the number of SAS data collection runs per object pose. Second, the number and types of objects were increased from the original UXO to include a 155-mm howitzer shell, 152-mm TP-T round, 82-mm finned mortar, solid AL and steel

replicas of the original UXO, two rocks of similar size (i.e., clutter), and the 2:1 AL cylinder. Third, six or more objects were placed in the field-of-view of the sonars. With multiple objects in a target field, techniques to isolate the scattering from a given object were required (see Sec. 4). Objects were again placed at 5 and 10 m horizontal ranges. Finally, a detailed description of PONDEX10 and the APL-UW rail-tower system is available in [1].

TREX13 represents a significant increase in the complexity of the experiment over that of the pond. First, this experiment was performed in the Gulf of Mexico south of Panama City, FL (~1 mile off shore). The sediment was a fairly flat medium-fine sand with a minor small-scale ripple field. Second, the rail was extended to a 42-m length with a usable 40-m SAS aperture. A 40×40 m^2 fixed grid was established in front of the rail. The SAS aperture allowed deployment of up to 30 objects in a target field with horizontal ranges from the rail of 5 to 40 m in 5 m increments. The primary frequency bands were 1-30, 30-50, and 110-190 kHz. With a water depth of ~17 m, maximum range of 40 m, and sonar height of ~4 m above the water-sediment interface, reflections from the air-water interface can be time-gated out of the data. Separation between adjacent objects was sufficiently large that multiple scattering can be ignored. Twenty-eight objects were available in TREX13 including 155-mm howitzer shells, 105-mm artillery shells with and without fins, the original UXO and its AL and steel replicas, the 2:1 AL cylinder, and a few clutter objects. Objects at the 5 m range were proud, partially buried, or fully buried. Objects at the 10 m range were either proud or partially buried. Objects were proud for all other ranges. Finally, the rail became an artificial reef in an otherwise flat underwater environment. Fish caused a significant increase in volume clutter.

BAYEX14 was conducted south of Panama City, FL in St. Andrew Bay, where the water is brackish with low visibility. The water depth was ~8 m, and the sediment consisted of a mud layer (15 to 30 cm thickness) over a sand subbottom. The 42-m length rail was again deployed with a 40×40 m^2 fixed grid. Horizontal ranges for object insertion coincided with those of TREX13. Objects from TREX13 were again used in BAYEX14. However, here, all objects were partially or fully embedded in the mud layer. For BAYEX14, two independent sonars simultaneously transmitted 1-30 and 110-190 kHz LFM pulses. The sonars were ~3.8 m above the subbottom (i.e., near mid water column). For the broad beamwidths of the sonars and horizontal ranges greater than a few water depths (e.g., > 20 m), reflections from the air-water interface cannot be neglected under calm conditions. Thus, environmental conditions of BAYEX14 presented a challenging increase in complexity.

CLUTTEREX17 returned to the site of TREX13. The 42-m long rail again was deployed, and simultaneous transmission of 1-30 and 110-190 kHz pulses were used during data collection. Here, the available objects increased to 68, where the inert UXO included 155-mm howitzer shells, 105-mm shells with and without fins, the 152-mm TP-T round, and the original UXO and its AL and steel replicas. Clutter objects included cement blocks, crab traps, lobster pots, boat anchors, small coolers, and rocks. In CLUTTEREX17, two types of experiments were conducted. First, 40×40 m^2 fixed grid was established, and targets were placed at locations similar to TREX13. Data were collected from targets only. Clutter objects then were inserted close to targets (i.e., typically < 1 m) and SAS data were recorded. Finally, targets were removed from the grid, and data were obtained for clutter objects only. The second type of experiment involved random target fields. Divers selected random objects and placed these object into a target field with random horizontal ranges and poses. Separation between adjacent objects in the initial target field was sufficient that the affect of one target on the acoustic target signature of another target was minimal. After data collection, divers were instructed to contract the target field where targets again have new random horizontal ranges and poses (i.e., target separation distances decrease). Contraction of the target field was repeated until the separation distance between neighbouring objects was ~1 m. Although the complexity of CLUTTEREX17 with respect to the environment is similar to that of TREX13, here an increase in complexity occurred due to the decreased separability of target acoustic signatures as the distance between targets is reduced.

3. NUMERICAL MODELS

Our experiments demonstrate that an acoustic response from an object depends on the environment and scattering geometry within that environment, so models must consider the target-in-the-environment. Two approaches to acoustic scattering from an object near the water-sediment interface have been pursued at APL-UW. These are the hybrid model and the target-in-the-environment response (TIER) model. Each is briefly described.

Many underwater UXO have cylindrical symmetry, which allows a decomposition of the full 3-D problem into a series of independent 2-D Fourier modal sub-problems. The hybrid model combines a 2-D finite-element (FE) model and a 3-D propagation model [1-3]. The 2-D FE model predicts the scattered pressure and derivatives on a discrete set of points closely surrounding an object. The pressure, derivatives, and an appropriate Green function are then used in a discrete form of the Helmholtz integral to propagate the scattered pressure to a distant receiver. The hybrid model is formulated in the frequency domain. As the hybrid model computes modal sub-problems, the modes of vibration of a target can be inspected. A superposition of the sub-problems, then allows one to obtain a complex-valued AC template. Thus, structure observed in an AC template can be directly attributed to an elastic response of the target in the environment.

Although advances in hardware and algorithms provide a reduction in the computational complexity of the hybrid model, it is still limited when large sets of data are required. The TIER model retains the high-fidelity of the hybrid model while providing a significant reduction in computation time. It combines an acoustic ray model for propagation and far-field scattering from an object in the free field (i.e., no boundaries) [4]. For the ray model, source and receiver are reflected through the boundaries of the waveguide to give a set of image sources and receivers. This effectively removes the boundaries and converts the scattering problem into a superposition of free-field scattering problems. Rays, associated with a source and its images, are scattered from an object. Scattered rays then propagate to the receiver and its images. Superposition of scattered rays yields the spectrum of the scattered pressure. Inverse Fourier transformation of the spectrum gives a time-domain signal (i.e., a sonar ping). The far-field scattered pressure has the form $p_s(\omega) = S(\boldsymbol{k}_i,\boldsymbol{k}_s,\omega)\exp(-i\omega t)/r$, where r is distance to a field point, the angular frequency is ω, and t is time. The scattering amplitude, $S(\boldsymbol{k}_i,\boldsymbol{k}_s,\omega)$, is a function of incident and scattered wave vectors $\boldsymbol{k}_i$ and $\boldsymbol{k}_s$ as well as ω. The scattering amplitude contains all of the information about an object (e.g., material properties) and the directionality of the scattered pressure. The hybrid model provided scattering amplitudes for the 2:1 and 3:1 AL cylinder, 155-mm howitzers, 105-mm artillery shells, AL and steel replicas of the original 4-in UXO, 2:1 open-ended AL pipe, and an oil drum. Comparisons to data and hybrid model results were used in the validation of the TIER model.

4. SIGNAL PROCESSING

Our signal processing steps include calibration, target isolation, and conversion of time-domain data to calibrated data products suitable for our classification schemes. Prior to an experiment, through-the-system calibrations of the sources, receivers, and electronics are performed. The calibration accounts for transmitter voltage response, receiver sensitivity, and characteristics of the electronic components (e.g., amplifier frequency response). Measured replicas of transmitted LFM pulses then are used during the pulse compression of the recorded data, where the system response is removed to give calibrated data. Target isolation and data products are then derived from the calibrated data as described in the following.

Although the rail provides a stable platform for the mobile tower to traverse, small-scale perturbations to straight-line motion occur. The small-scale motion causes a slight blurring in the SAS images, and affects HF SAS images more than LF images. A recent advancement in autofocusing of stripmap SAS images uses a collection of point-like glints and statistical metrics on contrast or sharpness to optimize for a phase correction [5]. This approach is applied to our HF data to obtain a phase correction. Simultaneous transmission of the LF and HF LFM pulses during BAYEX14 and CLUTTEREX17 allows for co-registration of LF and HF SAS images. Thus, HF phase correction can be applied to the LF SAS data.

Target isolation is performed by either synthetic aperture decomposition (SAD) [6] or holographic back-projection [7]. Both methods are essentially a spatial filtering of the data. The left panel in Fig. 1 shows an example of the isolated time signals after applying the SAD algorithm to data collected during TREX13 for a 2:1 AL cylinder. For SAD, an ω-k SAS algorithm converts the calibrated time-domain data into a complex-valued SAS image. A small region within the SAS image is preserved while all other parts are masked. Inverse SAS processing then converts the isolated portion of the SAS image back into the time-domain. With compensation for geometric spreading loss, the magnitude of the complex-valued SAS image is the absolute target strength (TS). The right panel is the full 360° AC template constructed from nine poses of the cylinder that span $-90° \leq \theta \leq 90°$.

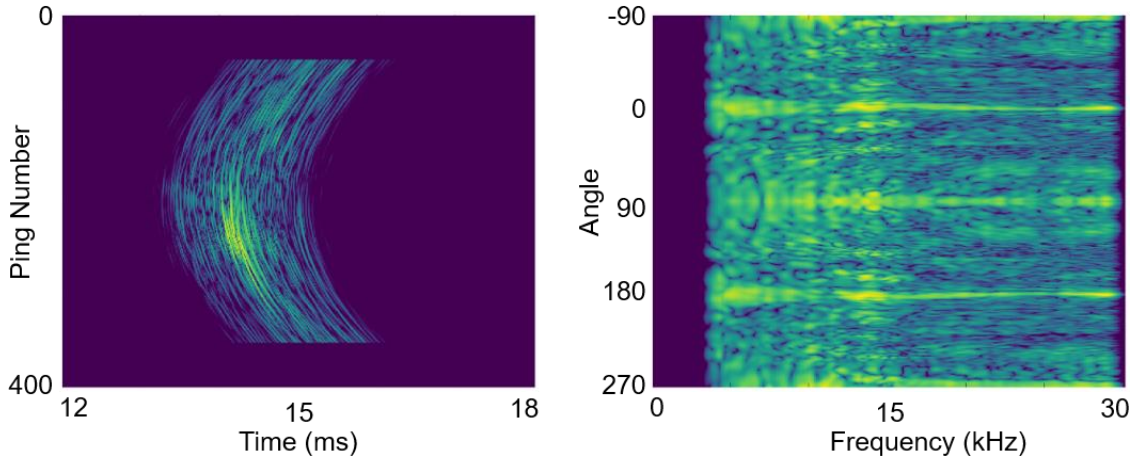

Fig. 1 Left: Time signature for scattering from a 2:1 AL cylinder. Right: Full AC template for the same cylinder. The data are from TREX13 with the cylinder at ~10 m range. The pings shown on the left correspond to approximately $-20° < \theta < 20°$ in the AC template.

The primary data products that we have used in our classification studies convert the time-domain data into AC templates. An AC template is the target strength as a function of target-centred aspect angle, θ, and frequency, f. For an axisymmetric target, an AC template spans $0° \leq \theta \leq 180°$ and $3 \leq f \leq 30$ kHz, where we typically have a 721×151 matrices. Three approaches have been developed. The first uses a template-matching scheme, based on cross-correlations of portions of AC templates (e.g., 40°×30 kHz or 81×151 matrix) and a relevance vector machine (RVM) classifier [8]. The second approach reduces the AC templates by an energy-based argument, where an AC template essentially is integrated over angular swaths and/or frequency bins [9]. Typically, this reduces the dimensionality of the data product from 81×151 to 1×18. The energy-based data products have been used with several classifiers available within MatLab™. The third approach trains a Gaussian mixture model (GMM) for each object, where individual angular values are randomly selected from its AC template (i.e., angular information within an AC template is lost) [10]. The GMM can be grouped to provide target vs non-target classification as well as be used in a multi-class situation to

distinguish one type of target from another (e.g., a 105-mm shell versus a 155-mm shell). Detailed discussion of the classification schemes is beyond this paper.

5. MULTI-SENSOR TOWBODY (MuST)

A limited-scope design study for an applied system was completed in 2016 [11], where it was determined that a towed platform was a cost-efficient option. The initial design includes both LF and HF sonars with additional electrical and communication capacity to support other sensors (e.g., magnetometers and optical devices). To reduce financial risk, the number of subsurface components is minimized such that the towboy control, signal generation, data collection, and data quality assessment are contained within a shipboard package. The left panel in Fig. 2 is an engineering design for the MuST displaying the LF source and receiver and the HF sonar. The right panel in Fig. 2 is a MacArtney Underwater Technology towbody, which was delivered to APL-UW in February 2019. The HF sonar is an EdgeTech 2205 side-scan sonar that can operate at 540 kHz and 1.6 MHz (giving sub-centimetre resolution for proud objects and sediment interface topology). The LF eBOSS sonar, also an EdgeTech product, is composed of one or more spherical radiators (5-35 kHz band width) and a 64-channel receiving array. Operationally, the eBOSS is a downward looking sonar, which offers ~1 m penetration into a sand sediment (~2 m for mud) for the detection of buried targets. Each channel of the receiving array is individually recorded. The shipboard package offers near real-time processing. It is anticipated that a 3-D image resolution of a 10×10×10 cm^3 voxel can be obtained with the eBOSS.

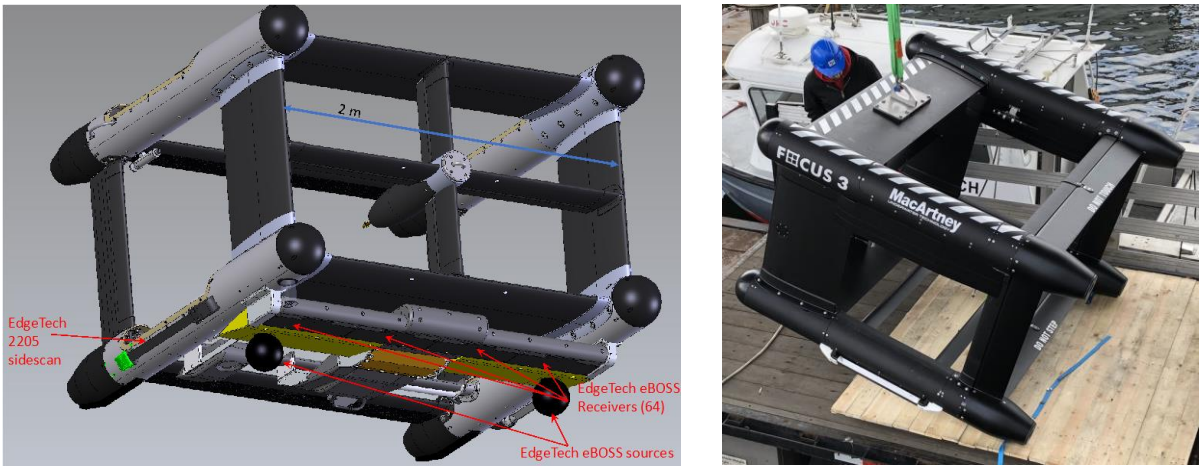

Fig. 2. Left: Engineering drawing of the MuST. Right: The MacArtney Focus 3 towbody. The LF omnidirectional sources and receivers comprise the EdgeTech eBOSS. The HF sonar is an EdgeTech 2205.

The MuST is designed to operate at a 5 m altitude above the water-sediment interface with a 100-200 m layout behind the ship. This altitude gives an ~19 m swath width for the eBOSS and ~30 m swath width for the HF side-scan sonar. Full coverage of an area of interest can be obtained with a mow-the-lawn survey and 15-m track spacing. An approximate area coverage rate of 0.1 km^2/hr is expected for a ship moving at 4 knots, where it is estimated that ~1 km^2 takes about 20 hr due to the necessary time for turning with a 200 m layout.

An initial wet test in Lake Washington and Puget Sound found that simple geo-location from reciprocal time-of-flight measurement and a 150 m layout gave ~3 m resolution with respect to absolute GPS geo-location. During the initial wet test, only the HF side-scan sonar was available. Data were collected for both the 540 kHz and 1.6 MHz frequencies. The eBOSS has been delivered to APL-UW and is currently undergoing calibration. A second test

is planned for Lake Washington in July 2019 where a single 2:1 AL cylinder will be deployed. Both LF and HF data are to be collected. The first test of MuST in an operational UXO remediation scenario is scheduled for September 2019 in Sequim Bay, WA. In this demonstration, two identical sets of objects will be deployed with one set placed in a sandy environment and one set placed in a muddy/silty environment. Each set will contain UXO (e.g., 155-mm howitzer), reference targets (e.g., 2:1 AL cylinder), and clutter objects (e.g., discarded scuba tanks).

6. SUMMARY

The transition of our basic research efforts into an applied platform to assist in UXO remediation is an on-going effort. The data collected from the five field experiments have been, and continue to be, used in validating two numerical models for target scattering. The numerical models then allow us to unravel the underlying target scattering physics by isolating mechanisms that lead to observable structure in data products derived from data. Both experimental data and simulated data were used in the training and testing of three approaches to classification. Each of these classification schemes have been integrated into software, which can be used for post mission analysis of a UXO remediation activity.

7. ACKNOWLEDGEMENTS

The research reported was jointly funded by the Strategic Environmental Research and Development Program (SERDP), the Environmental Security Technology Certification Program (ESTCP), and the Office of Naval Research (ONR). The experimental efforts were conducted in collaboration with the Naval Surface Warfare Center, Panama City Division. Both MacArtney and EdgeTech have been instrumental in overall MuST system definition and implementation.

REFERENCES

[1] **KL Williams, SG Kargl, EI Thorsos, DS Burnett, JL Lopes, M Zampolli, and PL Marston,** Acoustic scattering from a solid aluminum cylinder in contact with a sand sediment: Measurements, modeling, and interpretation, *J. Acoust. Soc. Am.*, 127, pp. 3356-3371, 2010.

[2] **M Zampolli, A Tesei, G Canepa, and OA Godin,** Computing the far field scattered or radiated by objects inside layered fluid media using approximate green's functions, *J. Acoust. Soc. Am.*, 123, pp. 4051-4058, 2008.

[3] **M Zampolli**, **AL España**, **KL Williams, SG Kargl, EI Thorsos, JL Lopes, JL Kennedy, and PL Marston**, Low- to mid-frequency scattering from elastic objects on a sand sea floor: simulation of frequency and aspect dependent structural echoes, *J. Comp. Acoust.*, 20, p. 1240007 (14 pp.), 2012, DOI: 10.1142/S0218396X12400073.

[4] **SG Kargl, AL Espana, KL Williams, JL Kennedy, JL Lopes**, Scattering from objects at a water sediment interface: Experiment, high-speed and high-fidelity models, and physical insight, *IEEE J. Ocean. Eng.*, 40, pp. 632-642, 2015.

[5] **TM Marston, DS Plotnick**, Semiparametric Statistical Stripmap Synthetic Aperture Autofocusing, *IEEE Trans. Geo. Remote Sensing.*, 53, pp. 2086-2095, 2015.

[6] **TM Marston, PL Marston, KL Williams**, Scattering resonances, filtering with reversible SAS processing, and applications of quantitative ray theory, In *Proc. 2010 OCEANS MTS/IEEE SEATTLE*, p. 9pp, 2010, DOI: 10.1109/OCEANS.2010.5664606.

[7] **DJ Zartman, DS Plotnick, TM Marston, PL Marston,** Quasi-holographic processing as an alternative to synthetic aperture sonar, *Proc. Mtgs on Acoust.,* 19, 5pp, 2013, DOI: 10.1121/1.4800881.

[8] **ME Tipping**, Sparse Bayesian Learning and the Relevance Vector Machine, *J. Mach. Learn. Res.*, 1, 211-244 (2001).

[9] **KL Williams, SG Kargl, AL España**, Use of time, space, frequency, and angle data products in understanding target-in-the-environment scattering physics, *J. Acoust. Soc. Am.*, 143, 1854, 2018.

[10] **CM Bishop**, Pattern Recognition and Machine Learning, (Springer, NY, 2006), Ch. 9. Sec. 2.

[11] **KL Williams**, Limited Scope Design Study for Multi-Sensor Tow Body, 2016, https://www.serdp-estcp.org/Program-Areas/Munitions-Response/Munitions-Underwater/MR-2501/MR-2501